


High sensitivity extended gate effect transistor based on V₂O₅ nanorods

N. M. Abd-Alghafour^{1,2}  · Naser M. Ahmed² · Z. Hassan² ·
Munirah Abdullah Almessiere³ · M. Bououdina⁴ · Naif H. Al-Hardan⁵

Received: 3 June 2016 / Accepted: 29 August 2016 / Published online: 24 September 2016
© Springer Science+Business Media New York 2016

Abstract The sensing characteristics of extended gate field effect transistor (EGFET) as pH sensor based on V₂O₅ nanorods (NRs) was fabricated for the first time. The as-deposited V₂O₅ NRs onto glass substrate by using spray pyrolysis method have a diameter of 140–160 nm and a length of 300–500 nm. The V₂O₅ NRs based EGFET pH sensor exhibited a remarkable pH sensing performance due to the larger effective sensing surface area. The sensing sensitivity and linearity of the pH-EGFET sensor was found to be 54.9 mV/pH and 0.9859, respectively in the range of pH 2–12. V₂O₅ NRs sensor showed superior pH sensing stability and reliability, thereby can be considered as potential candidate for mass fabrication in disposable biosensors.

1 Introduction

The field of research related to pH sensing has attracted great attention in particular in biochemical and biological applications. The ion-sensitive field effect transistor

technology (ISFET) based upon pH sensing was first fabricated by Bergveld in 1970s [1]. The current development in pH sensors is based on the development of extended-gate field effect transistor (EGFET) that represents in fact an alternative for the fabrication of ISFET [2, 3]. EGFET has revealed many features that overcome the traditional ISFET, such as flexible shape of the structure, low cost, temperature and insensitivity of the light, simpler packaging, and long stability [4, 5].

Several studies have been carried out to investigate the ion-sensing membranes of pH-EGFET based on various metal oxides thin films. Guerra et al. [6] obtained TiO₂ nanorods (NRs) by hydrothermal method at 150 °C for up to 50 h. As a sensing film on a pH-EGFET configuration, the NRs TiO₂ demonstrated a linear behaviour and a high sensitivity (49.6 mV/pH) for the pH range 2–12; 16 % below the theoretical limit (59.2 mV/pH). Lin et al. [7] fabricated EGFET pH sensor using ITO NRs onto Si substrate by photo-electrochemical technique. They found that the ITO NR structural EGFET pH sensors displayed high sensing performances owing to the larger sensing surface area. Li et al. [8] synthesized SnO₂ NRs as pH sensor. It demonstrated that SnO₂ NRs sensor exhibited a higher sensitivity (55.18 mV/pH) and larger linearity. Lee et al. [9] grew ZnO NRs array on the on the AlGaN/GaN heterostructure to combine as the ion-sensitive field-effect-transistor (ISFET) glucose biosensors. They concluded that the superior sensing performance compared with the other glucose biosensors. Guerra et al. [10] successfully synthesized EGFET based on vanadium pentoxide (V₂O₅) xerogel thin film using sole gel method. This xerogel demonstrated a linear behaviour and a high sensitivity of 58.1 mV/pH for the pH range of 2–10. It is important to highlight that the number of surface sites per unit area (N_s) affects the chemical sensitivity of the pH sensor [11].

✉ N. M. Abd-Alghafour
na2013bil@gmail.com

¹ Iraqi Ministry of Education, Anbar, Iraq

² Institute of Nano-Optoelectronics Research and Technology (INOR), Universiti Sains Malaysia, 11800 USM Penang, Malaysia

³ Department of Physics, College of Science, University of Dammam, Dammam, Kingdom of Saudi Arabia

⁴ Department of Physics, College of Science, University of Bahrain, P.O. Box 32038, Isa Town, Kingdom of Bahrain

⁵ School of Physics, Faculty of Science and Technology, Universiti Kebangsaan Malaysia, 43600 Bangi, Malaysia

Numerous studies have reported that the larger N_s , the high pH sensitivity and better linearity due to the higher sensing surface area [12, 13]. V_2O_5 exhibits excellent electrical and optical properties [10, 14], thereby can be considered as a promising candidate for wide range of applications such as gas sensor, window for solar cells, electronic devices and optical switches [15]. From the previous studies reported in literature, it is clear that V_2O_5 NRs have been rarely used to fabricate pH-EGFET sensor.

The EGFET involves three terminals; the source, drain, and gate. The voltage applied between the drain and source of EGFET controls the current drift in the gate voltage. Precisely, the current-control mechanism is based on an electric field created by the voltage applied to the gate. A positive voltage applied to the gate causes positive charges to be repulsed from the region of the substrate under the gate. These positive charges are pushed downward into the substrate, leaving behind a carrier-depletion region. The depletion region is populated by the bound negative charge related with the acceptor atoms. These charges are bared because the positive charges have been pushed downward into the substrate [16]. The positive gate voltage also pulls the negative charges from the substrate region into the channel region. When sufficient electrons are induced under the gate, an induced thin n-channel is in fact created, electrically bridging the source and drain regions. The channel is formed by inverting the substrate surface from p-type to n-type (inversion layer). The voltage is applied between the drain and source, current flows through this n-channel by the mobile electrons (n-type EGFET).

In this research work, we report on the fabrication of V_2O_5 NRs based pH-EGFET sensor. V_2O_5 NRs were synthesized by using low cost spray pyrolysis technique. The obtained results show high sensitivity and superior linearity, associated with larger areas for H^+ sensing provided by V_2O_5 NRs.

2 Experimental part

2.1 The V_2O_5 NRs preparation

V_2O_5 NRs were synthesized from vanadium chloride (VCl_3 , 99.9 %, Sigma Aldrich) by spray pyrolysis method, as described in the literature [17]. Abd-Alghafour et al. [18] studied the effect of varying solution concentration, deposition spray rate and substrate temperature on the evolution of structure, microstructure and optical properties. The paper presents studies related to growth nanorods, lengths, diameters and surface morphology in relation with different conditions. The precursor solution was prepared by dissolving 0.05 M of VCl_3 powder in 50 ml

solution of deionized water (Millipore, USA). Prior to deposition, the substrates were cleaned with a normal detergent by using ethanol and distilled water in ultrasonic bath for 20 min. V_2O_5 NRs were obtained under the following previously optimized experimental conditions: substrate temperatures $T_s = 350$ °C, distance 35 cm and spray rate of 5 ml/min.

2.2 Characterization techniques

The crystal structure of V_2O_5 NRs was studied by using high resolution XRD PANalytical X' pert Pro MRD diffractometer system equipped with Cu K α radiation ($\lambda = 1.54056$ Å) at 40 kV and 30 mA. The Raman spectrum was recorded using Jobin Yvon HR800UV with 514.5 nm emission at room temperature. Surface morphology of the film was examined by using field emission scanning electron microscopy (FESEM) (model FEI Nova NanoSEM 450) equipped with energy dispersive X-ray spectrometer (EDX) for chemical analysis. The electrical response of V_2O_5 NRs sensor was carried out by using different pH values from 2 to 12 and the measurements of the (I_{DS} – V_{DS}) were achieved by using an Agilent 4156C semiconductor parameter analyzer.

2.3 The sensor fabrication

The EGFET was fabricated using glass substrates with the dimensions of 2 cm \times 2 cm. The samples were attached to a strip of a copper clad laminate printed circuit board (PCB). After the V_2O_5 NRs growth, the silver paste served as the electrode was applied to the glass substrate. The metal conductive wire was bound with silver paste and packaged with epoxy resin. Subsequently, the packaged electrode was dried in an oven at 120 °C for 30 min. Epoxy resin was employed to define the sensing area of 0.3 cm \times 0.3 cm. Figure 1 presents the EGFET structure.

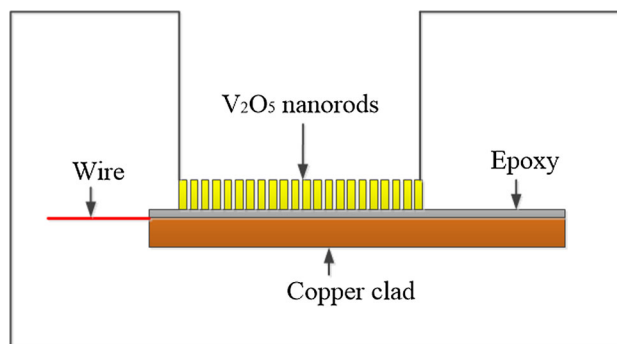


Fig. 1 Representation of the EGFET structure

2.4 Measurement processes

Figure 2 illustrated the pH sensing system setup; it consists of two Keithley 2400 source measure units (SMUs) (Keithley Instruments, Inc., Cleveland, OH, USA). The units were connected to a personal computer (PC) via a GPIB–USB cable, and LabTracer software (Keithley Instruments, Inc., Cleveland, OH, USA) was used to initiate the measurements and save the data for further analysis. A commercial Ag/AgCl reference electrode was adopted as the standard reference electrode, offering a constant potential during the whole measuring process. The sensing unit and the reference electrode were directly immersed into the buffer solution and electrically connected to the gate of commercial standard

MOSFET device (CD4007UB). To provide a stable reference voltage to the sensing element, a reference electrode was dipped into the same buffer solution and kept at room temperature (25 °C) for 2 min before the measurements. First the 2400 SMUs were employed to apply the drain–source voltage (V_{DS}) to the source and drain the terminals of the CD4007UB device and measure the drain–source output current (I_{DS}), while the second 2400 SMU was used to apply the reference voltage (V_{REF}) to the reference electrode.

3 Results and discussion

Figure 3 shows XRD pattern of V_2O_5 NRs. The as-deposited film reveals polycrystalline nature with an orthorhombic crystal structure. The peaks were indexed as (110), (101), (011), (301) and (002) reflections of the orthorhombic V_2O_5 crystal structure (JCPDS Card No. 00-001-0359) [19]. It is observed that the NRs have a preferred orientation along (110) direction which may be due to the recrystallization process favoured by the deposition temperature (pre-heated substrate).

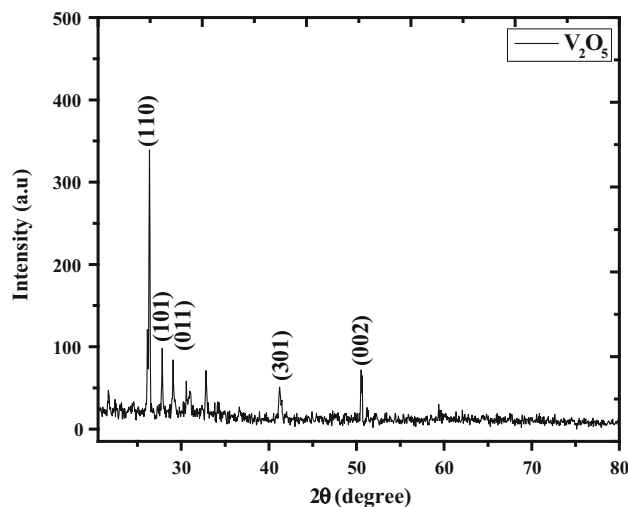
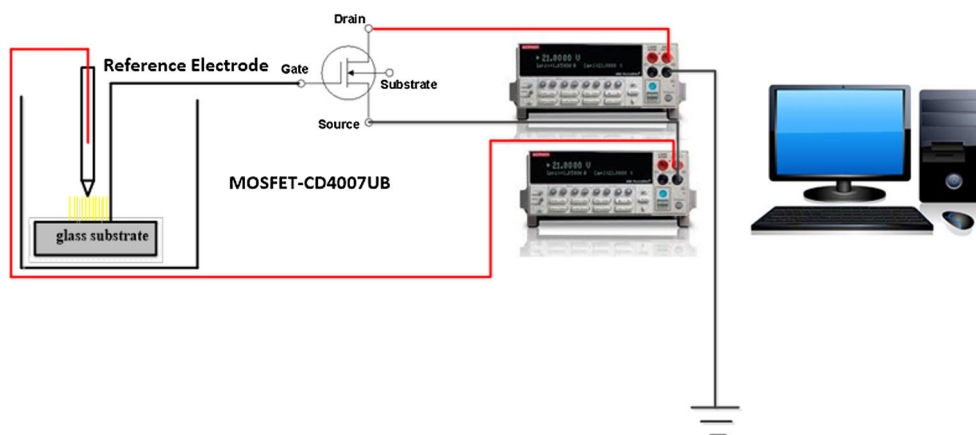


Fig. 3 XRD pattern of V_2O_5 NRs

The Raman spectrum of V_2O_5 NRs is displayed in Fig. 4. The intense peak at 143 cm^{-1} is associated with the vibrations of V–O–V chains, hence confirming the existence of layered orthorhombic structure of V_2O_5 phase. The intense peak located at 995 cm^{-1} corresponds to the terminal oxygen ($V^{+5} = O$) stretching mode that can be associated to the structural quality and stoichiometry of the as-deposited thin film [20]. In addition, a V_3O phonon mode is observed at 523 cm^{-1} along with the V–O–V mode at 696 cm^{-1} . The appearance of V–O–V mode was also confirmed by XRD analysis.

Figure 5a shows FESEM image of V_2O_5 NRs grown onto glass substrate. It can see large density and uniform growth of V_2O_5 NRs nearly perpendicular and randomly oriented to the glass substrate. The average diameter of NRs is around 150 nm and length of 500 nm, respectively. The thin film covered the large number of nucleation when the glass substrate surface was totally wrapped with intensive NRs. This high number of nucleation sites serves as a base for particle congregation. Moreover, the basic of NRs was generated

Fig. 2 Schematic diagram of EGFET pH sensor based on V_2O_5 NRs



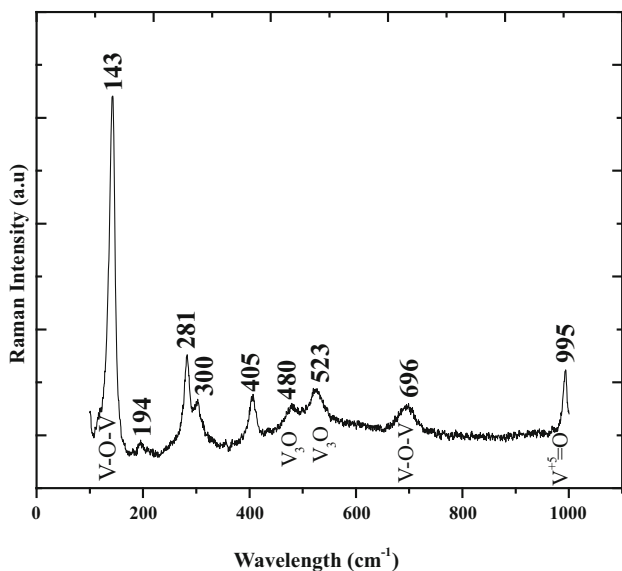


Fig. 4 Raman spectra of V₂O₅ NRs

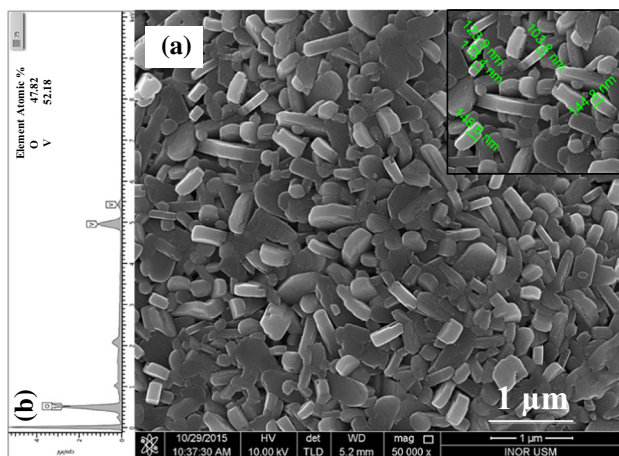


Fig. 5 V₂O₅ NRs grown onto glass substrate, a FESEM image, b EDX spectrum

through the coalescence of the as-congregated particles. Subsequently, the nanostructures grew with specific dimensions onto glass substrate surface through particles’ accumulation [21]. The proportions of V to O are revealed by the EDX spectrum shown in Fig. 5b. Chemical analysis gives 52.18 and 47.82 wt% of V and O, respectively, indicating better stoichiometry of the as-deposited film.

At the gate, the electric field is established by different pH values; the drain current variation of the EGFET can be used as the electrical response of pH sensor. Figure 6a displays the drain–source current (I_{DS}) versus drain–source voltage (V_{DS}) for V₂O₅ NRs based pH-EGFET sensor at $V_{REF} = 3.5$ V, $V_{DS} = 5$ V with various pH values. The results indicate that I_{DS} increases with the increase in pH value of the basic solution due to the aggregation of OH⁻, whereas I_{DS} decreases with increasing the pH value of the acid solution. From the

relation between I_{DS} and the pH value can be found using the basic MOSFET expression, where V_T is the threshold voltage related to the pH value. The value of saturation current is calculated from the relation [22]:

$$I_{DS} = \frac{\mu_n C_{ox}}{2} \times \frac{W}{L} [(V_{Ref} - V_T)^2 (1 + \lambda V_{DS})] \quad (1)$$

where μ_n the electron mobility in the channel, λ is the channel-length modulation factor, C_{ox} is the gate capacitance per unit area, W/L is the ratio of channel width-to-length, V_{Ref} and V_{DS} are the reference electrode and drain–source voltages. The square root of saturation current in Eq. (1) is given by:

$$\sqrt{I_{DS}} = \sqrt{\frac{\mu_n C_{ox}}{2}} \times \frac{W}{L} \times (1 + \lambda V_{DS}) \times (V_{Ref} - V_T) \quad (2)$$

Figure 6b shows the experimental $\sqrt{I_{DS}}$ versus pH values, for a $V_{Ref} = 3.5$ V and $V_{DS} = 5$ V. The results exhibit that the pH-EGFET has a greater linearly dependence over pH value in the saturation region. Accordingly, the sensitivity and linearity of V₂O₅ NRs based pH-EGFET sensor are 1.0414 $\mu A^{1/2}/pH$ and 0.9698, respectively. The drain–source current (I_{DS}) versus reference electrode voltage characteristics of V₂O₅ NRs based pH-sensor, in the linear saturation region operating at $V_{DS} = 0.3$ V, are shown in Fig. 7a. The obtained results indicate that the modified threshold voltage (V_T) depends upon the different pH value. The related V_T is defined as a reference electrode voltage when the drain–source current was shifted from zero mA. At $I_{DS} = 0.5$ mA, the reference electrode voltage at different pH values is obtained from CD4007UB MOSFET. Also, the I_{DS} – V_{REF} characteristic of V₂O₅ NRs is observed. The obtained reference electrode voltage versus pH value is shown in Fig. 7b. As a result, the V_{REF} depends linearly on the pH values in the saturation region. The sensing sensitivity and linearity of V₂O₅ NRs based pH-sensor are 54.9 mV/pH and 0.9859, respectively. Therefore, the pH-EGFET sensor based on V₂O₅ NRs can be considered as promising candidate for biosensors, such as urea and glucose sensors. Furthermore, Table 1 summarizes the sensitivity and linearity of some pH-EGFET sensors based on various nanostructures fabricated using different methods [6–10, 23, 24]. It can be seen that the as-fabricated pH-EGFET sensor reported in this study shows relatively comparable sensitivity and linearity. The mechanism of pH-EGFET sensor can be summarized as follows:

The basic principle of a pH-EGFET based dissolved oxygen sensor is the electrolysis of oxygen molecules. When the working electrode is held at the reduction potential of oxygen versus the reference electrode (anode), a sensor decreases an oxygen molecule at the working electrode (cathode) surface. They are two mechanisms of

Fig. 6 V_2O_5 NRs based EGFET pH sensor in the saturation region, **a** I_{DS} – V_{DS} characteristics, **b** sensitivity and linearity

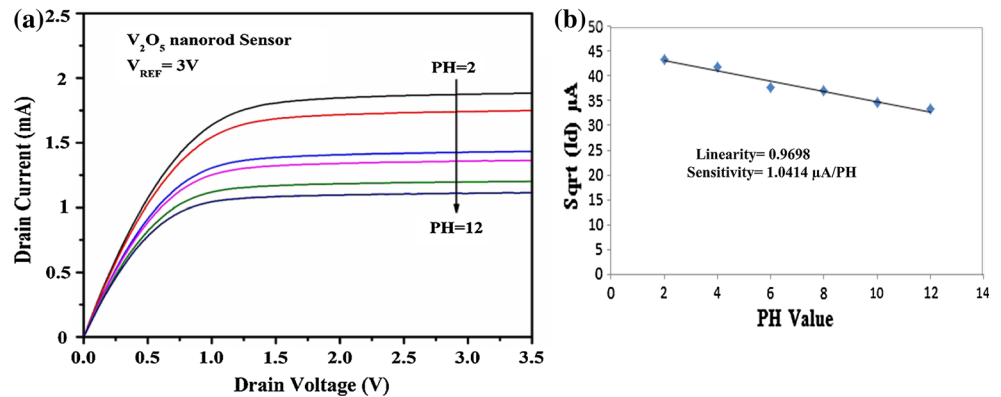


Fig. 7 V_2O_5 NRs structural EGFET pH sensor in the linear region, **a** I_{DS} – I_{REF} characteristics of, **b** sensitivity and linearity

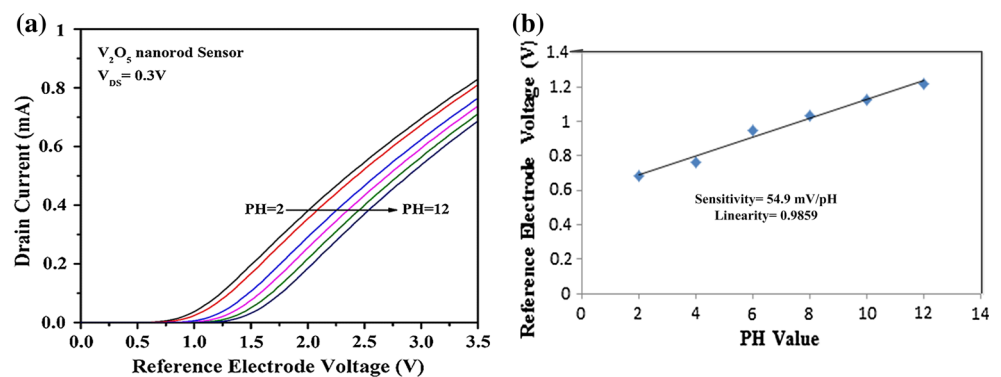
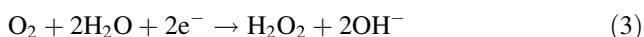


Table 1 Comparison of the sensitivity and linearity of the EGFET as pH sensor at different nanostructures

	Fabrication method	Sensitivity (mV/pH)	Linearity	References
TiO ₂ -NRs	Hydrothermal reaction	49.6	0.9592	[6]
ITO-NRs	VLS-electron beam	53.96	0.9839	[7]
SnO ₂ -NRs	Hydrothermally	55.18	0.9952	[8]
ZnO-NRs	PEC oxidation	57.66	0.9972	[9]
V_2O_5 -NRs	Spray pyrolysis	54.9	0.9859	This work
V_2O_5 -thin film	Sol-gel	58.1	0.9785	[10]
V_2O_5 -another nanostructure	Sol-gel	68	0.9986	[23]
V_2O_5 -another nanostructure	Hydrothermal reaction	38.1	0.9674	[24]

the oxygen reduction, one involving of two two-electron reactions with hydrogen peroxide as an intermediate:



And the other is a single four-electron reaction



Electrochemical current flows between the two electrodes, giving current output associated to the dissolved oxygen concentration. This current determines dissolved oxygen concentration. A pH change by the generation of hydroxyl ions (OH^-) as well as a current flow occurs

concurrently. A working electrode surrounding a pH-sensing gate of a pH-EGFET electrolyzes dissolved oxygen, resulting in a pH variation due to oxygen reduction in close proximity to the pH-sensing gate.

4 Conclusions

V_2O_5 NRs were synthesized by using spray pyrolysis technique. The V_2O_5 has an orthorhombic structure and NRs-like nanostructure having 140–160 nm diameter and 300–500 nm of length. The results show that V_2O_5 NRs sensor demonstrates a high sensitivity of 54.9 mA/pH and

superior linearity of 0.9859 in the saturation region. This could be attributed to the larger surface-to-volume ratio of the NR nanostructure which provides further surface sites and oxygen vacancies, indicating larger effective sensing areas. The as-fabricated V_2O_5 NRs pH EGFET sensor may be used as disposable biosensors.

Acknowledgments The authors gratefully acknowledge the financial support from the Universiti Sains Malaysia under RU Top Down Grant (1001/CINOR/870019).

References

1. P. Bergveld, Development of an ion-sensitive solid-state device for neurophysiological measurements. *IEEE Trans. Biomed. Eng.* **1**, 70–71 (1970)
2. M. Yuqing, C. Jianrong, F. Keming, New technology for the detection of pH. *J. Biochem. Biophys. Methods* **63**, 1–9 (2005)
3. L.-T. Yin, J.-C. Chou, W.-Y. Chung, T.-P. Sun, S.-K. Hsiung, Separate structure extended gate H⁺-ion sensitive field effect transistor on a glass substrate. *Sens. Actuators B: Chem.* **71**, 106–111 (2000)
4. J.-C. Chou, J.-L. Chiang, C.-L. Wu, pH and procaine sensing characteristics of extended—gate field-effect transistor based on indium tin oxide glass. *Jpn. J. Appl. Phys.* **44**, 4838 (2005)
5. N.H. Chou, J.C. Chou, T.P. Sun, S.K. Hsiung, Differential type solid-state urea biosensors based on ion-selective electrodes. *Sens. Actuators B: Chem.* **130**, 359–366 (2008)
6. E.M. Guerra, M. Mulato, Titanium oxide nanorods pH sensors: comparison between voltammetry and extended gate field effect transistor measurements. *Mater. Sci. Appl.* **5**, 459–466 (2014)
7. T.-S. Lin, C.-T. Lee, H.-Y. Lee, C.-C. Lin, Surface passivation function of indium-tin-oxide-based nanorod structural sensors. *Appl. Surf. Sci.* **258**, 8415–8418 (2012)
8. H.-H. Li, W.-S. Dai, J.-C. Chou, H.-C. Cheng, An extended—gate field-effect transistor with low-temperature hydrothermally synthesized nanorods as pH sensor. *IEEE Electron Device Lett.* **33**, 1495–1497 (2012)
9. C.-T. Lee, Y.-S. Chiu, Photoelectrochemical passivated ZnO—based nanorod structured glucose biosensors using gate—recessed AlGaIn/GaN ion—sensitive field-effect—transistors. *Sens. Actuators B: Chem.* **210**, 756–761 (2015)
10. E.M. Guerra, G.R. Silva, M. Mulato, Extended gate field effect transistor using V_2O_5 xerogel sensing membrane by sol–gel method. *Solid State Sci.* **11**, 456–460 (2009)
11. J.-L. Chiang, Y.-C. Chen, J.-C. Chou, Simulation and experimental study of the pH—sensing property for AlN thin films. *Jpn. J. Appl. Phys.* **40**, 5900 (2001)
12. C.-T. Lee, Y.-S. Chiu, S.-C. Ho, Y.-J. Lee, Investigation of a photoelectrochemical passivated ZnO-based glucose biosensor. *Sensors* **11**, 4648–4655 (2011)
13. A. Fulati, S.M. Usman Ali, M. Riaz, G. Amin, O. Nur, M. Willander, Miniaturized pH sensors based on zinc oxide nanotubes/nanorods. *Sensors* **9**, 8911–8923 (2009)
14. C.A. Brunello, C.F. Graeff, H.P. Oliveira, Synthesis, characterization, and conductivity studies of poly-o-methoxyaniline intercalated into V_2O_5 xerogel. *J. Solid State Chem.* **168**, 134–139 (2002)
15. H.P. Oliveira, C.F. Graeff, C.A. Brunello, E.D.M. Guerra, Electrochromic and conductivity properties: a comparative study between melanin-like/ $V_2O_5 \cdot nH_2O$ and polyaniline/ $V_2O_5 \cdot nH_2O$ hybrid materials. *J. Non Cryst. Solids* **273**, 193–197 (2000)
16. D.G. Pijanowska, W. Torbicz, Biosensors for bioanalytical applications. *Tech. Sci.* **53**(3), (2005)
17. A. Mane, V. Ganbavle, M. Gaikwad, S. Nikam, K. Rajpure, A. Moholkar, Physicochemical properties of sprayed V_2O_5 thin films: effect of substrate temperature. *J. Anal. Appl. Pyrol.* **115**, 57–65 (2015)
18. N. Abd-Alghafour, N.M. Ahmed, Z. Hassan, S.M. Mohammad, M. Bououdina, M. Ali, Characterization of V_2O_5 nanorods grown by spray pyrolysis technique. *J. Mater. Sci. Mater. Electron.* **27**, 4613–4621 (2016)
19. Z. El Mandouh, M. Selim, Physical properties of vanadium pentoxide sol gel films. *Thin Solid Films* **371**, 259–263 (2000)
20. L.-J. Meng, R.A. Silva, H.-N. Cui, V. Teixeira, M. Dos Santos, Z. Xu, Optical and structural properties of vanadium pentoxide films prepared by DC reactive magnetron sputtering. *Thin Solid Films* **515**, 195–200 (2006)
21. A.M. Selman, Z. Hassan, Highly sensitive fast-response UV photodiode fabricated from rutile TiO_2 nanorod array on silicon substrate. *Sens. Actuators, A* **221**, 15–21 (2015)
22. L.-L. Chi, J.-C. Chou, W.-Y. Chung, T.-P. Sun, S.-K. Hsiung, Study on extended gate field effect transistor with tin oxide sensing membrane. *Mater. Chem. Phys.* **63**, 19–23 (2000)
23. E.M. Guerra, M. Mulato, Synthesis and characterization of vanadium oxide/hexadecylamine membrane and its application as pH-EGFET sensor. *J. Sol Gel Sci. Technol.* **52**, 315–320 (2009)
24. E.J. Guidelli, E.M. Guerra, M. Mulato, V_2O_5/WO_3 mixed oxide films as pH-EGFET sensor: sequential re-usage and fabrication volume analysis. *ECS J. Solid State Sci. Technol.* **1**, N39–N44 (2012)